Statistical simulations of diffusional coarsening in finite clusters

H. Mandyam and M. E. Glicksman
Department of Chemical Engineering, Rensselaer Polytechnic Institute, Troy, New York 12180-3590

J. Helsing
Department of Solid Mechanics, Royal Institute of Technology, SE-100 44 Stockholm, Sweden

S. P. Marsh
Physical Metallurgy Branch, Naval Research Laboratory, Washington, D.C. 20375-5343
(Received 29 October 1996; revised manuscript received 4 March 1997)

The problem of diffusional interactions in a finite-sized cluster of spherical particles is studied. Simulations of diffusional interactions with size distribution and volume fraction V_v, as input parameters, referred to as snapshot (static) simulations, are compared with dynamic (time-dependent) simulation results. The precise size distribution information in the snapshot simulations is obtained on the basis of a perturbation technique proposed recently by Fradkov *et al.* [Phys. Rev. E **53**, 3925 (1996)]. Robust iterative solution schemes for the quasistatic diffusion equation facilitate investigations of coarsening systems comprised of one million particles at ultralow (10^{-13}) to moderate (0.25) volume fractions. The objective of carrying out simulations at such low volume fractions is to analyze the first-order volume-fraction-dependent correction to the effective coarsening rate predicted by the Todes, Lifshitz, and Slyozov (TLS) theory at infinite dilution. When volume fraction is considered as an input parameter, the deviation of coarsening rates from that of the infinite dilution limit of TLS varies as $\sqrt[3]{V_v}$ for a finite cluster and $\sqrt{V_v}$ (Debye screening) for an infinite system. Accurate numerical investigations of the rollover volume fraction (V_v^*) above which the $\sqrt[3]{V_v}$ behavior changes to $\sqrt{V_v}$ showed that V_v^* varies as n^{-2}, where n is the number of particles in the spherical cluster. The deviation of coarsening rates from TLS observed from dynamic simulations agrees with that predicted by snapshot simulations for $V_v < 0.01$. The dynamic results are higher than the snapshot results for $V_v > 0.01$. The coarsening rate of the average particle can be calculated directly from dynamic simulations and indirectly from snapshot simulations by a perturbation relation. A different type of snapshot-ensemble averaging is suggested on the basis of the functional nature of the individual particle monopole source or sink strengths. Dynamic and snapshot simulations with dipoles were carried out up to a volume fraction of 0.25, and departure from Debye screening behavior was observed. The inclusion of dipole terms affects the deviations noticeably only above a volume fraction of 0.1. [S1063-651X(98)02208-9]

PACS number(s): 82.30.−b

I. INTRODUCTION

Diffusional coarsening represents an important kinetic process in the late stage of phase separation. This process characterizes the microstructural evolution of dispersed precipitates in a matrix phase. The asymptotic limit of this evolution is described by the theories of Lifshitz and Slyozov [1] and Todes (TLS) [2]. These theories, however, describe coarsening at infinitesimally low volume fractions. At finite volume fractions, there is a deviation in the average coarsening rate from that of the TLS theory. The increase in coarsening rates is expected because the TLS theory does not take into account any interactions among particles. Experiments have shown that as the volume fraction increases, the amplitude of the temporal power law for the average particle size, i.e., the rate constant, rises. The particle size distribution function becomes broader and more symmetrical than that predicted by the TLS theory. The concentration gradient at the particle/matrix interface is expected to increase progressively with volume fraction. It has been established that the exponent of the temporal power law remains unchanged at a nonzero volume fraction, but the rate constant increases [3].

The influence of a nonzero volume fraction of the coarsening phase has been investigated through mean-field theories [4–7] and statistical field theories [8,9] and by numerical simulations [10–12]. Marder's theory [13] yields a rate constant at a particular volume fraction that is higher than those predicted by other theories. The analytical theory of Marqusee and Ross [8], based on the diffusion analog of Debye screening for infinite systems, leads to deviations of coarsening rates proportional to $\sqrt{V_v}$. On the other hand, several other numerical analyses of finite systems clearly show that the relative change in the rate constant is proportional to $\sqrt[3]{V_v}$. A recently published paper by Fradkov, Glicksman, and Marsh [14] shows the existence of both exponents of volume fractions, using numerical simulations of a finite cluster of particles. They specifically solved the quasistatic diffusion field for a finite cluster of particles with the size distribution and volume fraction as input parameters. This type of simulation, also referred to as snapshot simulation, is less time consuming than the conventional time-dependent simulations. Their work, however, had the limitations of computing the behavior of clusters with less than a thousand particles with limited statistical samples. This paper extends their perturbation theory and simulations to larger systems and larger ensembles to determine accurately the rollover

volume fraction at which diffusional interactions of the order of the diffusion Debye length become comparable with interactions of the order of the cluster size that characterizes the spatial extent of the cluster. Further, in this paper we also report time-dependent simulations in the volume fraction range $10^{-12}<V_v<0.25$ and compare the results with those obtained from snapshot simulations.

The numerical simulations by Akaiwa and Voorhees [15] show spatial correlation effects on coarsening of particles placed in a periodic array, with or without solute depletion zones. Although experimental measurements [16,17] of structure factors and spatial correlation functions have not directly established the presence of solute depletion zones, some researchers [18–20] have attempted to reproduce structure factors by assuming that particles are surrounded by a spherical depletion zone. Krichevsky and Stavans [21] experimentally established that the probability of finding smaller particles near larger ones is greater than that of finding smaller and larger ones near each other. Recently, the same authors [22] also discuss the direct correlation and medium polarization effects based on their experimental investigations on two-dimensional microstructures comprised of a crystalline phase dispersed in a continuous melt phase.

This paper is organized as follows. In Sec. II, we describe the mean-field formulation of the problem of coarsening of spherical particles to dipolar order. This is followed by Sec. III, wherein we present some kinetics of finite coarsening clusters and briefly discuss the perturbation theory that forms the basis of the snapshot simulations. In Sec. IV, we describe in detail our simulation techniques (snapshot and dynamic) and also present our analytical findings as regards quantities of physical interest. The words ''particles,'' ''droplets,'' and ''precipitates'' are used interchangeably throughout the paper.

II. MEAN-FIELD APPROACHES

The description of isothermal coarsening is given in terms of a dimensionless concentration potential, ϕ, that satisfies the Laplace equation

$$\nabla^2\phi=0. \tag{1}$$

The boundary conditions at the surface of the ith particle having a radius R_i are specified through the Gibbs-Thomson local equilibrium relation

$$\phi_i=\frac{\lambda}{R_i}, \tag{2}$$

where λ is a capillary length defined by

$$\lambda=2\frac{\gamma\Omega}{k_BT}. \tag{3}$$

Here, γ is the specific interfacial free energy, Ω is the molar volume, k_B is Boltzmann's constant, and T is the absolute temperature. The solution to the Laplace equation (the exterior Dirichlet problem) to dipolar order for n particles can be represented as

$$\phi(\mathbf{r})=\sum_{i=1}^{n}\frac{\lambda B_i}{|\mathbf{r}-\mathbf{r}_i|}+\sum_{i=1}^{n}\lambda\mathbf{d}_i\cdot\nabla\left(\frac{1}{|\mathbf{r}-\mathbf{r}_i|}\right)+\phi_\infty. \tag{4}$$

The monopole strengths B_i's, the dipole strengths $\mathbf{d}_i$'s, and the far field potential ϕ_∞ are the unknown coefficients to be determined using the other boundary conditions of the problem. The assumption of a quasistatic diffusion field leads to the following time rate of change of the particle radius:

$$v(R_i)=\frac{-2\lambda D_0c_0B_i\Omega}{R_i^2}, \tag{5}$$

where D_0 is the diffusion coefficient and c_0 is the equilibrium solubility. The size distribution function $F(R,t)$ follows a Fokker-Planck-type equation in size-time space. Here we do not consider the effect of noise or residual matrix supersaturation, and thus the conservation equation may be approximated as

$$\frac{\partial F}{\partial t}+\frac{\partial(v(R)F)}{\partial R}=0. \tag{6}$$

The unknown size distribution function is normalized as

$$\int_0^\infty F(R,t)dR=N_v, \tag{7}$$

where N_v is the number of particles per unit volume. With this normalization the volume fraction V_v is defined as

$$V_v\equiv\frac{4\pi}{3}\int_0^\infty F(R,t)R^3dR, \tag{8}$$

hence

$$V_v=\frac{4\pi}{3}N_v\langle R^3\rangle. \tag{9}$$

The diffusion potential at a particle-matrix interface arising from the self-field and the fields of other particles can be expanded in a Taylor series [23] around the particle center as

$$\frac{\lambda}{R_i}=\left(\phi_i^*+\phi_\infty+\frac{\lambda B_i}{R_i}\right)+\left(\nabla\phi_i^*+\frac{\lambda\mathbf{d}_i}{R_i^3}\right)\cdot\mathbf{R}_i+\cdots+(\text{higher-order terms}). \tag{10}$$

For Eq. (10) to possess solutions for any particle and direction in space, we require for the scalar terms

$$\frac{\lambda}{R_i}=\phi_i^*+\phi_\infty+\frac{\lambda B_i}{R_i}, \tag{11}$$

and for the vector terms

$$\nabla\phi_i^*+\frac{\lambda\mathbf{d}_i}{R_i^3}=\mathbf{0}. \tag{12}$$

Here, ϕ_i^* is the potential created by all other particles at the center of the ith particle and is given by

$$\phi_i^*(\mathbf{r}) = \sum_{j\neq i=1}^{n} \frac{\lambda B_j}{|\mathbf{r}_j - \mathbf{r}_i|} + \sum_{j\neq i=1}^{n} \lambda \mathbf{d}_j \cdot \boldsymbol{\nabla}\left(\frac{1}{|\mathbf{r}_j - \mathbf{r}_i|}\right) \quad (13)$$

and

$$\boldsymbol{\nabla}\phi_i^*(\mathbf{r}) = \sum_{j\neq i=1}^{n} \boldsymbol{\nabla}\frac{\lambda B_j}{|\mathbf{r}_j - \mathbf{r}_i|} + \sum_{j\neq i=1}^{n} \lambda \mathbf{d}_j \cdot \boldsymbol{\nabla}\boldsymbol{\nabla}\left(\frac{1}{|\mathbf{r}_j - \mathbf{r}_i|}\right). \quad (14)$$

Further, for a conservative coarsening system, strictly in the asymptotic stage (again neglecting any residual supersaturation) the volume fraction constraint over the dispersed phase may be written in integral form as

$$\frac{4\pi}{3}\int_0^\infty \frac{\partial F(R,t)}{\partial t} R^3 dR = 0. \quad (15)$$

Equation (15) can be written for a discrete system of particles as

$$\sum_{i=1}^{n} B_i = 0. \quad (16)$$

The TLS limit of the same problem attributes an infinite extent to the diffusion field of a single particle, thus giving to monopolar order the analytic form

$$B_i = \left(1 - \frac{R_i}{R^*}\right), \quad (17)$$

where R^* is the critical particle radius, the interface potential of which matches the far-field potential and is given by

$$R^* = \lambda/\phi_\infty. \quad (18)$$

Todes introduced a dimensionless variable transformation $\rho = R/R^*$. The dimensionality of diffusion-limited coarsening implies that kinetically the critical radius behaves as

$$R^* = \alpha(2\lambda D_0 c_0 \Omega t)^{1/3}, \quad (19)$$

where α is a dimensionless kinetic coefficient that can be determined from the Lifshitz and Slyozov [1] stability analysis. Todes also suggested a family of self-similar solutions for the distribution function $F(R,t)$, given by

$$F(R,t) = \frac{N_v(t)}{R^*(t)} f(\rho,\alpha). \quad (20)$$

Substituting Eq. (20) and $B^{\mathrm{TLS}} = (\rho - 1)$ into the conservation equation and using separation of variables to solve the eigenvalue problem with the help of Eq. (8), we get

$$\rho[(3/\alpha^3)(1-\rho) + \rho^3]\frac{\partial f}{\partial \rho} + [-4\rho^3 + (6/\alpha^3)](1-\rho/2) f = 0. \quad (21)$$

This can be rewritten in separated form as

$$\frac{df}{f} = \frac{-4\rho^3 + (6/\alpha^3)(1-\rho/2)}{(3/\alpha^3)(1-\rho) + \rho^3}\frac{d\rho}{\rho} \quad (22)$$

for the time-independent part of the size distribution in the TLS case. Here we have treated B as a continuous function of ρ. Note that in [14] the equation corresponding to Eq. (22) has a typographical error.

The stability argument of Lifshitz and Sloyozov [1] states that for the size distribution to be self-similar, there exists a maximum particle radius $\rho^{\max}$ in ρ space for which the time rate of change in ρ space follows,

$$\left[\frac{d\rho}{dt}\right]_{\rho^{\max}} = 0 \quad (23)$$

and

$$\left[\frac{\partial}{\partial \rho}\frac{d\rho}{dt}\right]_{\rho^{\max}} = 0. \quad (24)$$

The above two conditions can also be restated in terms of the denominator of Eq. (22), $D = (3/\alpha^3)(1-\rho) + \rho^3$. Lifshitz and Slyozov stated that the only stable solution of the continuity equation corresponds to a value of α, which makes the positive roots of the denominator coincide. This implies that $\alpha_{\mathrm{TLS}} = (2/3)^{2/3}$.

There are different approaches to incorporate the effect of volume fraction on coarsening. Some researchers have restricted the interparticle spacing to the average interparticle separation. In systems that are not sparse, direct screening by nearest neighbors becomes important, and closest particle correlations begin to develop [3]. Marqusee and Ross [8] restricted the extent of the Laplacian field by taking into account screening in a two-phase medium consisting of a distribution of sources and sinks. This leads to the Poisson equation for the spatially coarse-grained background diffusion potential ϕ, namely

$$\nabla^2\phi = -4\pi\sigma, \quad (25)$$

where the source or sink density σ is given by

$$\sigma(\mathbf{r}) = \int_0^\infty [\lambda - R\phi(\mathbf{r})] F(R,t) dR. \quad (26)$$

The background potential ϕ_∞ has been replaced by the coarse-grained ϕ, giving the linearized form of the Poisson-Boltzmann equation, also known as the Debye-Hückel equation:

$$\nabla^2\phi - \kappa^2(\phi - \phi_\infty) = 0. \quad (27)$$

In Eq. (27),

$$\kappa^2 = 4\pi\langle R\rangle N_v \quad (28)$$

and

$$\phi_\infty = \lambda/\langle R\rangle. \quad (29)$$

The Debye-Hückel equation is well known from theories of ionic plasma and electrolytes. The solution to this equation, subject to the Gibbs-Thomson boundary condition, is of the form of a Yukawa potential

$$\phi(\mathbf{r}) = \sum_{i=1}^{n} \lambda \frac{B_i}{|\mathbf{r}-\mathbf{r}_i|} e^{-\kappa|\mathbf{r}-\mathbf{r}_i|} + \phi_\infty . \tag{30}$$

Now the B_i's are defined as

$$B_i = \left(1 - \frac{R_i \phi_\infty}{\lambda}\right)(1+\kappa R_i) = B_i^{\mathrm{TLS}}(1+\kappa R_i). \tag{31}$$

The coefficient κ is the reciprocal of the diffusion analog of the screening length. It represents the natural cutoff distance for the direct particle interactions via the diffusion field, beyond which the particles are isolated from each other by the intervening two-phase medium. This, however, is not the same as the diffusion depletion distance proposed by Rikvold and Gunton [19] or by Pedersen's curve fitting analysis of SANS data [18]. The screening length represents the distance beyond which particles do not diffusionally interact with each other. Interactions within this distance can be broken down into single-body and many-body diffusional interactions. In order to incorporate the effect of the volume fraction, Tokuyama and Kawasaki [24] used hierarchy equations to describe many-body diffusional interactions. The equations they obtained were in general different from the familiar BBGKY hierarchy equations for molecular distribution functions [25]. Diffusional interactions between particles in a finite cluster can be represented as hard-sphere interactions coupled with solute depletion zones [18,19]. Pedersen specifically modeled coarsening particles as Percus-Yevick hard spheres encapsulated in a solute depletion zone of size proportional to the hard-sphere radius itself. This method precisely described structure factors in sintering experiments [20]. The random field cell approach developed by Marsh and Glicksman [3] proposed a diffusion depletion distance for each particle as the radial distance at which the spherically symmetric Laplacian potential of that particle matches the mean-field potential. This approximation also suggested a one-to-one correspondence between particles and matrix field cells surrounding them.

III. KINETICS OF FINITE COARSENING CLUSTERS

The length scales of a finite coarsening cluster, i.e., a finite number of particles confined to a finite volume, are important factors in determining the kinetic properties of coarsening systems. The four important length scales in a finite coarsening cluster are [14] the size of the particles, as characterized by the average radius $\Lambda_R \approx \langle R \rangle$; the interparticle spacing as characterized by $\Lambda_N \approx N_v^{-1/3}$; the Debye screening radius as characterized by $\Lambda_D \approx \kappa^{-1}$; and the extent of the total coarsening system, defined for a spherical cluster as $\Lambda_{\mathrm{tot}} = (3n/4\pi N_v)^{1/3}$, where n is the number of particles in the cluster. It is assumed that the cluster is locally homogeneous and spatially isotropic, and that the overall size of the cluster is time independent. Therefore, one can define the volume fraction of a cluster of particles to be

$$V_v = \frac{\sum_{i=1}^{n} (4/3)\pi R_i^3}{(4/3)\pi(\Lambda_{\mathrm{tot}})^3}. \tag{32}$$

A finite system of coarsening particles, in contrast to an infinite system, cannot show *uniform* asymptotics, because any finite coarsening system achieves its end state as a single particle in finite time. Finite systems, however, may show *intermediate* asymptotics only. By this we mean that the coarse-grained average over time of these cluster parameters becomes identical to those in self-similar infinite systems, even though the instantaneous values of the time-dependent cluster parameters may fluctuate. In general, continuum coarsening theories yield quantities that are equivalent to the coarse-grained averages over time for finite clusters. Hence, the coarse-grained intensive length scale parameters, viz., Λ_R, Λ_N, and Λ_D can be expected to scale with time as predicted by continuum theories.

In finite systems, as observed in [11,26,15], coarsening occurs via continuous evolution of particle radii and by the discontinuous disappearance of the smallest particles. The coarse-grained averages depend on both mechanisms. The objective of simulating coarsening in finite clusters is to compute the coarsening rate. This can be found from the slope of the evolution of $\langle R \rangle$ with time. The coarse-grained behavior should show smooth $t^{1/3}$ behavior, which is in agreement with the asymptotic power law of continuum theories. In order to obtain a smooth time dependence, a large number of particles have to be simulated. If the objective is to determine the volume fraction dependence of the average rate constant of coarsening, then a time-dependent simulation would be needed for an enormously large number of particles at different volume fractions. This approach would pose a computationally intensive task. The task would be made considerably easier if the size distribution and volume fraction could be obtained or assumed *a priori* at each volume fraction. The multiparticle diffusion equation could then be solved instantaneously to calculate the average rate constant of coarsening.

In order to obtain the size distribution at low volume fractions, one can approximate it as a perturbation of the TLS distribution. The particle growth rate at finite volume fractions can be written as a perturbation of that at infinitesimally low volume fraction as done in [14] as

$$v(R) = v_{\mathrm{TLS}}(R)[1+\epsilon(R)], \tag{33}$$

where $\epsilon(R)$ is a small perturbation. If the perturbation is from Debye screening, then $\epsilon(R) = \kappa R$. Marqusee and Ross [8] used the same stability analysis as Lifshitz and Slyozov to obtain the kinetic constant corresponding to Debye screening as

$$\alpha(V_v) = \alpha_{\mathrm{TLS}}[1 + 0.740 V_v^{1/2} + (\text{higher-order terms})], \tag{34}$$

where $\alpha_{\mathrm{TLS}} = (2/3)^{2/3}$. Fradkov *et al.* [14] used the same stability analysis to arrive at a more general perturbation result as follows: If the denominator in Eq. (22) is perturbed, then

$$D = \rho^3 - \beta(\rho-1)(1+\epsilon), \tag{35}$$

where $\beta = 3/\alpha^3$. The eigenvalue for β and the maximum value of ρ can be found for solving the equation set $D=0$ and $D'=0$ [14]. To obtain first-order corrections to the eigenvalue, we write

$$\beta=\beta_{\mathrm{TLS}}+\delta\beta \tag{36}$$

and

$$\rho=\rho_{\mathrm{TLS}}+\delta\rho. \tag{37}$$

Retaining first-order terms we have

$$D=-\delta\beta/2-27\epsilon/8=0, \tag{38}$$

where $\rho_{\mathrm{TLS}}^{\max}=3/2$. This results in $\delta\beta=-27\epsilon/4$. Hence

$$\alpha=\alpha_{\mathrm{TLS}}[1+(3/16)^{1/3}\epsilon(R_{\max}^{\mathrm{TLS}})] \tag{39}$$

and

$$\rho^{\max}=\rho_{\mathrm{TLS}}^{\max}+(3/8)\epsilon', \tag{40}$$

where $\epsilon'=\partial\epsilon/\partial\rho$. Fradkov *et al.* used a snapshot simulation technique that indirectly assumed an $\epsilon(\rho)$ value for each particle in the finite cluster and then averaged the perturbations over the entire system of particles, using the assumption that the global average $\langle\epsilon(\rho)\rangle$ reflects the behavior of $\epsilon(\rho^{\max})$. This implies that the magnitude of the growth rate for each particle size class in a cluster is uniformly magnified relative to the TLS values. A more consistent refinement to this approximation is presented in the next section and yields more accurate values for ϵ for a given volume fraction. In this paper, we also extend this global average to several realizations of the system of particles in finite clusters.

Diffusional interactions in a cluster can be considerably influenced by noise in the system and by centroid migration of particles. Voorhees and Schaefer [27] considered the interaction between a pair of particles with a background potential ϕ_∞. They computed the interfacial velocities in the normal direction analytically to dipolar order as

$$V_n^1=(1/R_1)\{\phi_\infty-1/R_1+(1/R_2-\phi_\infty)R_2/2d-R_1R_2/4d^2 \times[1/R_1-\phi_\infty+3(1/R_2-\phi_\infty)\cos\theta]\}. \tag{41}$$

In Eq. (41), R_1 and R_2 are the particle radii and d is the interfocal separation as defined in [27]. The $\cos\theta$ term clearly suggests that the particle translates in the $\vec{n}\cos\theta=\vec{k}$ direction at a speed

$$V_T^1=-3/4d^2[1-R_2\phi_\infty]. \tag{42}$$

For an n-particle system, however, the leading-order term of the migration velocities [13] is

$$\mathbf{V}_T^i=\mathbf{r}_i=\frac{-\mathbf{d}_i}{R_i^3}. \tag{43}$$

Migration of particles in a cluster can result in the development of time-dependent correlations. Higher-order interactions of particles result in shape change, particularly flattening of approaching interfaces. The influence of hydrodynamic interactions on the coarsening rate of droplets combining through diffusive coalescence was studied by Siggia [28]. It was concluded that for low droplet volume fractions the evaporation-condensation mechanism proposed by Lifshitz and Slyozov is dominant. Further, the rate of coalescence is diminished by the effects of surface deformations and flattening of approaching interfaces in the late stage of phase separation.

IV. NUMERICAL SIMULATION AND RESULTS

In this section we solve Eqs. (1) and (2) numerically for a dispersion of coarsening spheres with two different approximations for the potential ϕ: (i) a monopole representation and (ii) a monopole plus dipole representation.

Snapshot simulations were done by choosing a particular size distribution at a given volume fraction and solving for the diffusion field of the given number of particles in the spherical cluster of radius Λ_{tot}. The geometry was created by assigning positions to the particles using the procedure of random sequential addition of hard spheres into a spherical cell [29]. Each particle was assigned a radius randomly distributed around the average value of the radius $\langle R\rangle=\lambda_R$. We specifically chose the TLS and rectangular size distributions of different widths. The numerical results obtained were relatively insensitive to the size distribution used for $V_v<0.01$. The ratio $\Lambda_R/\Lambda_{\mathrm{tot}}$ as defined in the preceding section was varied to obtain different volume fractions according to Eq. (26). We maintained the same relative particle positions over the range of volume fraction $V_v<0.01$, but proportionally changed the interparticle distances and thus changed the size of the cluster. For higher volume fractions ($V_v\geqslant 0.10$) we further modify this method as explained later in this section.

Inserting a solution of the form of Eq. (4) into Eqs. (1) and (2) leads to $[4n+1]\times[4n+1]$ linear equations. The condition number for this problem is large, but can be reduced by rewriting the problem as two systems of $[4n]\times[4n]$ linear equations. Furthermore, each of these smaller systems is positive definite and was solved iteratively with a preconditioned conjugate-gradient method suggested by McFadden and Greengard [30]. The relative error was set to a value of 10^{-4} at $V_v=0.10$ and progressively reduced at lower volume fractions to 10^{-7} at $V_v=10^{-14}$. Calculations involving n monopoles only led to systems of $[n+1]\times[n+1]$ linear equations and were solved in a similar manner. The number of realizations used was chosen so that an ensemble of at least a million spheres was involved in the calculations at each volume fraction studied.

Dynamic simulations were performed by choosing an initial size distribution and an arbitrary number of particles, solving for the diffusion field and subsequently time marching the radius of each particle according to Eq. (5). In order to account for particle disappearances, we chose a cutoff radius, below which a particle is considered to be nonexistent. Time marching was done to obtain a final desired number of particles coarsening in the asymptotic regime. The above procedure was repeated for several initial realizations and the results averaged out. The method of numerical solution was the same as that used for the snapshot simulations.

We performed the dynamic simulations with a particle cutoff radius of 0.05 times the maximum radius and with 1500 particles in the initial ensemble. Time marching was done to obtain an average of 500 particles coarsening in the asymptotic regime. The asymptotic regime is characterized by the cubic power-law behavior of the average particle radius of the cluster, such as $\langle R\rangle^3\sim t$, as shown in Fig. 1.

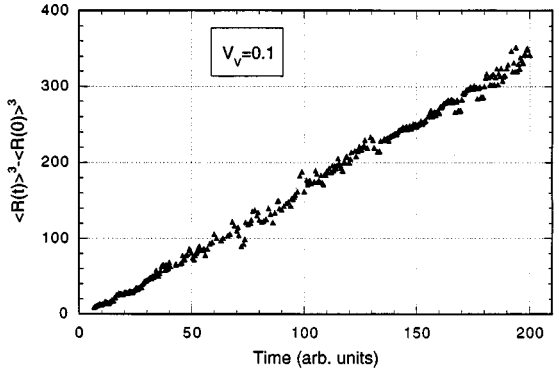

FIG. 1. Asymptotic power law of coarsening.

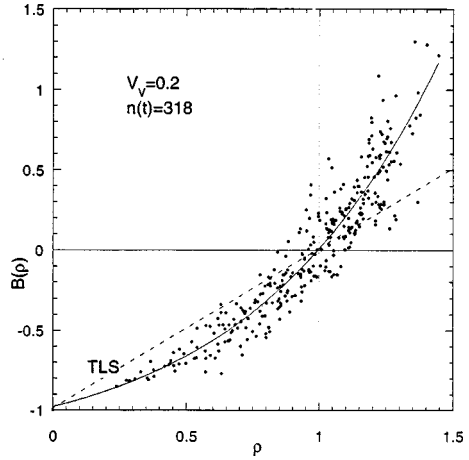

FIG. 2. Functional form of $B(\rho)$ showing noise distribution around the least-squares polynomial fit. $B(\rho)$ for $\rho \geq 1$ is almost linear for $V_v = 0.2$. $n(t)$ denotes the number of particles in the cluster.

In order to understand the basis of the snapshot simulation technique, we focus attention on the quantity Δ. The deviation Δ of the coarsening rate from the TLS limit ($V_v = 0$) is given as

$$\Delta(V_v) = \frac{\langle v(R,V_v)\rangle - \langle v(R,0)\rangle}{\langle v(R,0)\rangle}. \tag{44}$$

The above definition originates from averaging Eq. (33) as

$$\frac{\langle v(R)\rangle - \langle v_{\mathrm{TLS}}\rangle}{\langle v_{\mathrm{TLS}}\rangle} = \frac{\langle v_{\mathrm{TLS}}\epsilon(R)\rangle}{\langle v_{\mathrm{TLS}}\rangle} \tag{45}$$

and noting that v_{TLS} and $v(R,0)$ have been used interchangeably. The right-hand side of the above equation can also be thought of as an ensemble average of the volume fraction induced perturbations in the growth rate of the particles from a known set at another volume fraction. This quantity can be calculated at an instant for a system of coarsening particles with a given size distribution and at a known volume fraction. In principle, one can substitute the TLS distribution with any other known distribution at a nonzero volume fraction and ensemble average the perturbations at that volume fraction.

The value $\Delta(V_v)$, thus obtained, is substituted into Eq. (39) and hence the ratio $\alpha/\alpha_{\mathrm{TLS}}$ can be calculated. The absolute rate constant of the average particle is then

$$K = \alpha^3 = \frac{d}{dt}\,(R^{*3}). \tag{46}$$

Hence $K/K_{\mathrm{TLS}} = (\alpha/\alpha_{\mathrm{TLS}})^3 = [1 + (3/16)^{1/3}\Delta]^3$ can in principle be calculated for a given volume fraction once the deviation $\Delta(V_v)$ at that volume fraction is known. Henceforth we unambiguously refer to $\Delta(V_v)$ as the deviation in coarsening rates, and to K as the coarsening rate of the average particle. The value of K can also be obtained directly from the slope of the $\langle R\rangle^3$ vs t plot in a time dynamic simulation.

The principal assumption made here is that the global average $\langle \epsilon(R)\rangle$ reflects the behavior of $\epsilon(R_{\mathrm{max}})$. This assumption is necessary since a finite coarsening cluster does not have a statically valid representation of enough particles at R_{max}. The definition of $\Delta(V_v)$ in terms of a global average over a large statistical ensemble of particles makes it possible to get accurate estimates of coarsening rates. Using a single global average $\epsilon(R)$ implies that the B_i values increase uniformly in magnitude for all radii values at a given volume fraction. This is equivalent to assuming that the $B(\rho)$ vs ρ plot of Fig. 2, which is a straight line for the TLS theory, remains a straight line and that only the slope changes. There are two fixed points in this plot for $B(\rho)$: $B(1) = 0$, defining the critical particle size, and $B(0) = -1$, independent of volume fraction, caused by field localization for disappearing particles that approximate monopoles. Thus the function $B(\rho)$ becomes curved for shrinking particles in order to have a larger slope near $\rho = 1$ yet pass through these two fixed points. Coarsening theories and simulations [10,11,3], however, have shown that the $B(\rho)$ function remains nearly linear for growing particles ($\rho \geq 1$). Thus $\langle \epsilon(R)\rangle$ is essentially constant for ($\rho \geq 1$), and a more reliable estimate of this parameter used to determine $\Delta(V_v)$ can be obtained by averaging the individual ϵ values only for the growing particles in a given cluster.

If the deviation Δ from Eq. (44) is computed at different times for a given volume fraction, we can study the time dependence of $\Delta(V_v;t)$. This quantity will also show different branches of constant particle number with vertical jumps associated with particle disappearance. A smoother dependence can be obtained by coarse-graining the data. The coarse-graining was done by binning the $\Delta(V_v;t)$ data in time and representing each bin by its average value. In doing so, we are averaging over the different branches of constant particle number and the vertical jumps from each branch. A comparison of coarse-grained values of $\Delta(V_v;t)$ calculated for an average over *all* particles, with Δ obtained by averaging over *growing* particles only, in Fig. 3, clearly suggests that the average over growing particles alone is more stable and also closer to the snapshot values calculated by the snapshot simulation technique.

If Δ is given a stochastic description, then we need to associate a finite mean and variance with it. From Fig. 3, Δ for $\rho \geq 1$ has the snapshot value as its mean. The next objective now is to find a way to assign its variance appropriately. In this paper, ensemble averaging of these snapshots was used to get its variance. Although this serves our current purpose, a better estimate of the variance can be obtained by solving a non-Markov type Fokker-Planck equation for the

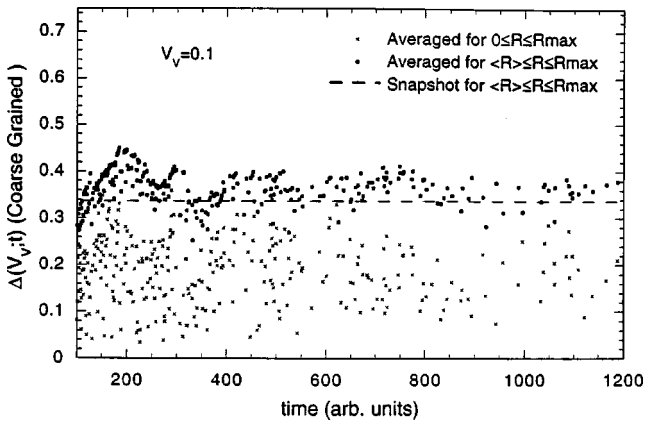

FIG. 3. Coarse-grained deviation from TLS vs time. Coarse graining was done by binning the data points and representing each bin by its time average. The snapshot value was calculated from the known size distribution at $V_v = 0.10$.

particle growth rates. Enomoto and Tokuyama [31] have used a similar method for studying phase separation. Yet another approach is to obtain the noise functional relationship for $B(\rho)$ vs ρ, with or without volume fraction as a parameter, and employ stochastic decomposition techniques. Preliminary studies confirm the non-Gaussian nature of the variance of the $B(\rho)$ data from the best-fit polynomial function (see Fig. 2). Such studies, however, do not affect the volume fraction exponents of coarsening rates and shall not be treated here.

The deviations in coarsening rates were computed in the volume fraction range $10^{-14} \leqslant V_v \leqslant 0.01$. The deviation values were found to agree with the Debye screening results of Fradkov, Glicksman, and Marsh [14], who used a first-order perturbation analysis to arrive at the expression

$$\Delta = \left(\frac{1-\mu_{-1}}{\mu_1 - \mu_{-2}} \right) \left(\frac{3}{\mu_3} \right)^{1/2} V_v^{1/2}. \tag{47}$$

Here the μ_i's are the ith moments of the size distribution with both shrinking and growing particles taken into account, and

$$\mu_i = \frac{\int_0^\infty R^i F(R,t)\,dR}{\langle R \rangle^i N_v}. \tag{48}$$

For the TLS distribution,

$$\Delta = 0.695 V_v^{1/2}. \tag{49}$$

The above equation is only a first-order approximation at nonzero volume fractions, given that the size distribution itself is broader than the TLS distribution. Strictly, one must use Eqs. (33) and (34) and solve for the size distribution from Eq. (21). Marqusee and Ross [8] have obtained such corrections to the TLS size distribution by using the diffusion analog of Debye screening at much higher volume fractions.

Snapshot simulations were carried out with n chosen to be 100, 316, 1000, and 3162, limited to monopoles in the volume fraction range $10^{-14} \leqslant V_v \leqslant 0.01$. The number of realizations were chosen so as to statistically simulate a total of a million particles. Such large ensembles of particles had to be realized in order to reduce the variance in Δ. We found that the deviation of coarsening rate from TLS showed a $V_v^{1/3}$ behavior at low volume fractions and a $V_v^{1/2}$ dependence at higher volume fractions, as shown in Fig. 4. The transition or rollover from the $\frac{1}{3}$ to the $\frac{1}{2}$ behavior was found to occur at V_v^*, which depended on the number of particles as

$$V_v^* \sim \frac{1}{3n^2}. \tag{50}$$

The V_v^* for the 3162 particle case was graphically estimated by the point of intersection of a line of slope $\frac{1}{3}$ through the point $(10^{-14}, \Delta(10^{-14}))$ and the line $\Delta = 0.695 V_v^{1/2}$ in Fig. 4. The number of particles in the cluster and the corresponding number of realizations used for averaging are also shown in Fig. 4.

In order to understand why the rollover behavior occurs, we look at the expressions for the cluster size and the Debye length,

$$\Lambda_D = 3^{-1/2} \left(\frac{\langle R^3 \rangle}{\langle R \rangle} \right)^{1/2} V_v^{-1/2} \tag{51}$$

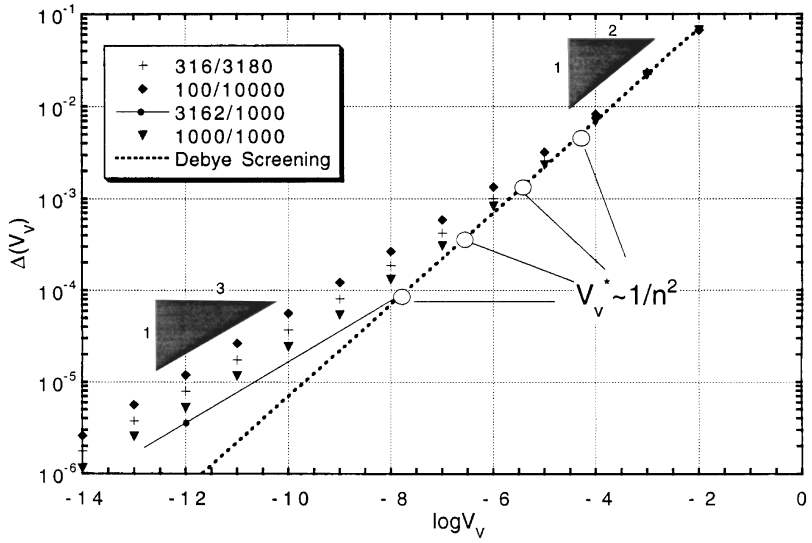

FIG. 4. Deviations in snapshot coarsening rates at low volume fractions. The numbers such as 316/3180 mean that diffusion fluxes were computed for 316 particles in a single cluster and the results statistically averaged over 3180 realizations and so on. The open circles indicate the rollover points where the slope changes from 1/2 to 1/3.

and

$$\Lambda_{\rm tot} = n^{1/3}\langle R^3\rangle^{1/3} V_V^{-1/3}. \tag{52}$$

The above equations show that the Debye length grows faster than the cluster size with decreasing volume fraction. This implies that at some small volume fraction V_v^*, the Λ_D exceeds the cluster size, and hence diffusion Debye screening is precluded. At such low volume fractions, one can estimate the diffusion fluxes by considering the monopole terms only, and we obtain

$$B_i - B_{\rm TLS} = -\frac{R_i}{\lambda}\left[\sum_{j=1\neq i}^{n} \frac{B_j}{|\mathbf{r}_j - \mathbf{r}_i|}\right].$$

The right-hand side of the above equation can be estimated using the appropriate length scales defined in Sec. III. Hence,

$$\frac{B_i - B_{\rm TLS}}{B_{\rm TLS}} \approx \frac{\Lambda_R}{\Lambda_N} = \frac{\langle R\rangle^{1/3}}{\langle R^3\rangle} V_v^{1/3}.$$

This shows that for extremely sparse clusters, the leading-order deviation from TLS kinetics goes as $V_v^{1/3}$. Thus, the rollover behavior occurs at some volume fraction for which the interactions at the order of the cluster size become comparable with those at the order of the Debye length. Equating these interactions gives the approximate condition

$$\Lambda_D(n, V_v^*) \approx \Lambda_{\rm tot}(n, V_v^*). \tag{53}$$

Hence

$$V_v^* \sim \frac{1}{27n^2}. \tag{54}$$

The difference in the constants appearing in Eqs. (54) and (50) can be related to an edge effect, which is precluded in the length scale argument. An edge effect may be inherent to finite clusters, since particles close to the outer regions of the cluster have fewer neighbors than those deep within the interior. We discuss this subtle effect in the subsection on periodic clusters.

For volume fractions greater than 0.01, one expects the deviation values to gradually become sensitive to the nature of the size distribution and spatial correlations developed through time evolution. In order to test the validity of the snapshot simulation technique for $V_v \leq 0.01$, a cluster of 2000 initial particles at $V_v = 0.02$ was time marched until the asymptotic stage of coarsening was reached with 500 particles remaining in the cluster. At this instant the particle positions and radii were recorded. Now the ratio $\Lambda_R/\Lambda_{\rm tot}$ for this cluster was suitably changed to obtain a cluster of 500 particles at lower volume fractions in the range $10^{-13} \leq V_v \leq 0.01$. The deviation Δ at each volume fraction was calculated from Eq. (44). Comparison of the deviations calculated in this manner with those calculated by directly time marching the cluster at each volume fraction yielded good agreement. More precisely, the dynamic simulation predicted $\Delta(0.01) = 0.0698 \pm 0.0015$ whereas the snapshot simulation result was $\Delta(0.01) = 0.0688$. Both these values are close to the perturbation theory value of 0.0695. At much lower volume fractions, the agreement was even better. Thus, given a time-marched system of particles in a finite cluster at a given volume fraction, one can estimate the deviation, Δ. Thus, the average coarsening rate constant at lower volume fractions can be estimated accurately by way of snapshot simulations, avoiding tedious dynamic simulations at lower volume fractions.

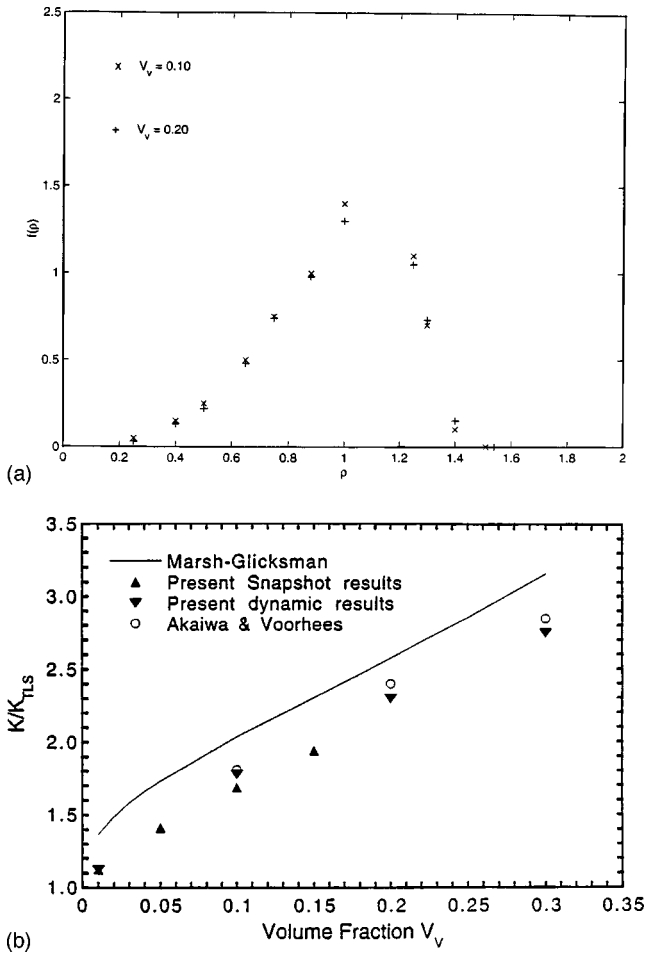

FIG. 5. (a) Scaled particle size distribution. (b) Comparison of coarsening rates at different volume fractions. The snapshot results are based on averaging over growing particles alone.

In order to check if such a conclusion can also be reached at volume fractions higher than 0.01, some dynamic and snapshot simulations were carried out in the volume fraction range $0.01 < V_v < 0.2$. Specifically, we considered an already time-marched cluster of 500 particles at $V_v = 0.2$, and changed the ratio $\Lambda_R/\Lambda_{\rm tot}$ to obtain a cluster of 500 particles at $V_v = 0.1$. The radii of the particles were distributed around the average value of the radius in a manner similar to that used in the former volume fraction and assigned the same relative positions as before. In doing so, we perturb the size distribution and recalculate the corresponding diffusional fluxes consistent with Eq. (45). Figure 5(a) shows the scaled particle size distribution $f(\rho)$ at $V_v = 0.2$ and 0.1, obtained from time dynamic simulations. The snapshot simulation technique assigns the radii for particles at $V_v = 0.1$, according to $f(\rho)$ at $V_v = 0.2$, but taking into account the resultant change in $\rho^{\rm max}$. This procedure follows the methodology of the perturbation technique. The change in $\rho^{\rm max}$ is recorded automatically in a snapshot simulation. This is true because

we move from one volume fraction branch of the B vs ρ plot to another branch corresponding to a lower volume fraction. The almost linear nature of the B vs ρ curve (Fig. 2) for growing particles shows that the kinetics of the growing particles is well captured by the snapshot simulations. The only significant errors in the snapshot simulations would be those arising from time evolved spatial correlations and the precise nature of the size distribution, both of which are unique to the asymptotic stage of each volume fraction. The use of different configurations at the original volume fraction $V_v = 0.20$ is bound to lead to different particle coarsening rates at $V_v = 0.10$. Hence, one needs to carry out some averaging over the configurations at $V_v = 0.10$. This was again done by random sequential addition of the particles into the same cluster volume. This averaging can be done over enough realizations to obtain a reasonably accurate estimate of the deviation Δ. The calculated value of the deviation was $\Delta(0.1) = 0.316$. In terms of the average rate constant values, $K(0.1)/K_{\mathrm{TLS}} = 1.772 \pm 0.033$ for a directly time-marched cluster, whereas $K(0.1)/K_{\mathrm{TLS}} = 1.622$ for a cluster that has been snapshot simulated at this volume fraction. If the ensemble averaging were to be carried out for particles in the range $1 < \rho < \rho^{\max}$, then $\Delta(0.1) = 0.336$ and the corresponding $K(0.1)/K_{\mathrm{TLS}} = 1.696$. We believe that the small relative difference in these values from the snapshot and dynamic simulations occurs because the time-evolved spatial correlations at each volume fraction are unique. In other words, the local environment in which a particle finds itself is different at different volume fractions. A more detailed explanation of this point could be given in terms of structure factors and nearest-neighbor distributions, and is part of an ongoing study to be reported elsewhere. A similar comparison at a volume fraction of 0.01 yielded a value of $\Delta(0.01) = 0.0698 \pm 0.0015$ for a directly time-marched cluster and a value of $\Delta(0.01) = 0.0687$ for a cluster obtained as a snapshot at this volume fraction. At volume fractions beyond about $V_v \geqslant 0.1$, we expect spatial correlation effects to be important. At these intermediate volume fractions the coarsening rates are sensitive to the precise nature of the size distribution and its time-evolved correlations.

In fact, snapshot simulations based on imprecise size distributions at the higher volume fractions have led to deviations and average coarsening rates that are much different from those obtained directly from dynamic simulations as in [32]. Hence, snapshot simulations may not be a reliable tool for predicting accurately the coarsening rates at moderately high volume fractions, especially if the precise nature of the size distribution and spatial correlations is not incorporated at the original volume fraction. Nonetheless, snapshot simulations result in accurate predictions for $V_v \leqslant 0.01$. In Fig. 5(b), a comparison is shown of time-dynamic simulation results with the results of previous simulations by Akaiwa and Voorhees [15] and the random field cell model by Marsh and Glicksman [3]. The theory in [3] incorporates a diffusional interaction distance for each particle in a matrix volume that has a certain specified correlation with the particle volume. The results of this theory are about 20% higher than the present simulation results. Also, this theory yields a $V_v^{1/3}$ dependence for Δ for an infinite system at low volume fractions.

We also performed snapshot simulations including dipole terms in the potential formulation for clusters containing 100 particles to determine the relative significance of dipolar interactions compared to monopolar interactions at low volume fractions. Again at low ranges of volume fraction the exponent of the volume fraction was $\frac{1}{3}$, and at higher values it was found to be $\frac{1}{2}$.

The dipolar contributions became significant only when $V_v \geqslant 10^{-2}$. Thus the exponents of the volume fraction do not change with the addition of dipole terms in the volume fraction range $10^{-14} \leqslant V_v \leqslant 0.01$. In order to understand the relative significance of the dipole terms at volume fractions higher than 0.01, we performed snapshot simulations of 1000 particles in a spherical cluster in the volume fraction range $0.02 \leqslant V_v \leqslant 0.20$. Our objective is to calculate the increase in deviation caused by the dipole terms alone. The difference $\Delta_{M+D} - \Delta_M$ between the deviations for the case with monopoles and dipoles (Δ_{M+D}) and that with monopoles only (Δ_M) was computed for 1000 particles. The difference showed a $V_v^{0.68 \pm 0.02}$ dependence at volume fractions close to 0.2 and a $V_v^{0.56 \pm 0.02}$ dependence at volume fractions close to 0.02. Hence we conclude that the inclusion of dipolar interactions results in a small positive departure from the $V_v^{1/2}$ behavior. We also noted that at these volume fractions, the coarsening rates were more sensitive to the size distribution used, in contrast to the relative insensitivity observed at low volume fractions. Particle migration rates were also computed from Eq. (43), but the migration neither changed the volume fraction exponents nor other qualitative conclusions. At higher volume fractions, however, spatial correlations were affected by particle centroid migration.

The proposition that the particles themselves are not hard spheres but have around them a hard concentric shell is known to impose another length scale corresponding to a solute depletion zone. The effect of depletion zones and spatial correlations on the deviations from TLS has been discussed by some researchers. Rikvold and Gunton [19] propose a depletion zone given as $V_v^{-1/3} - 1$. The simulations by Akaiwa and Voorhees [15] and the structure factor fits of Pedersen [18], however, use a depletion zone of 0.5 times the radii of the particles. Pedersen's work demonstrated that a model with both particle correlation and polydispersity effects can be used for interpreting small-angle scattering data from precipitates in alloys. He used a polydisperse hard-sphere model based on analytical expressions by Vrij [33] and produced good fits of structure factor data using R_{hs}, a hard-sphere radius, as one of the parameters. The understanding here is that every particle along with its concentric outer sphere of influence can be characterized by a hard sphere of radius R_{hs}. The corresponding hard-sphere volume fraction V_v^{hs} is simply related to the precipitate volume fraction by

$$V_v = V_v^{\mathrm{hs}} \Big/ \left(\frac{R_{\mathrm{hs}}}{R} \right)^3 . \tag{55}$$

In our specific case of $R_{\mathrm{hs}} = 1.5R$, we have $V_v = V_v^{\mathrm{hs}}/3.375$. We performed simulations with depletion zones of 0.5 times the radii and found that the Δ values from simulations as shown in Fig. 6 were slightly lower than in the case without

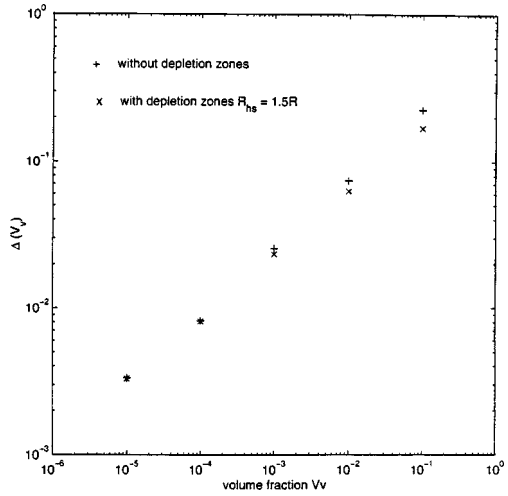

FIG. 6. Influence of depletion zones on deviations in coarsening rates from TLS.

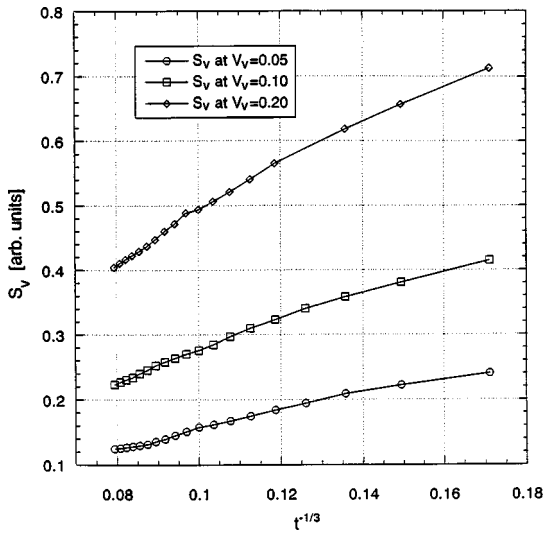

FIG. 7. Time dependence of interfacial area per unit volume.

any depletion zones for the volume fraction range of 0.1 to 10^{-14}. The dependence of the deviation Δ was still $V_v^{1/3}$ in the ultralow volume fraction range and $V_v^{1/2}$ in the upper range shown in Fig. 6. The rollover precipitate volume fraction still depends on the number of particles in the cluster as $V_v^* \sim 1/n^2$. Thus a depletion zone does not significantly alter the diffusional interactions of the order of the interparticle distance as well as the Debye length. The only noticeable effect was that the rollover volume fraction V_v^* is larger than that for cases without depletion zones by a multiplicative factor between 3 and 4. Accurate numerical estimation of V_v^* showed that the same factor was $3.70 \pm 0.33 \approx 1.5^3$. This calculation needed an accuracy of a very high order. When we used a depletion zone with $R_{\rm hs} = 1.8R$, we again found the factor to be $6.10 \pm 0.33 \approx 1.8^3$. In order to get more accurate estimates, one needs to implement variance reduction techniques such as importance sampling [34]. Based on the present simulation results on slope estimates, we find that the rollover precipitate volume fraction for the case with depletion zones, $V_v^{*\rm DZ}$, is related to the rollover volume fraction without depletion zones as $V_v^* \approx V_v^{*\rm DZ}/(R_{\rm hs}/R)^3$. There is, however, a limit to the size of the depletion zone that can be used for a given number of particles at a given volume fraction in a finite cluster, the limit being that of close-packing in hard spheres [35,36]. The depletion-zone radii proposed by Rikvold and Gunton are difficult to analyze at these low volume fractions. This is so because it is not possible to place a fixed number of particles with large depletion zones in a finite cluster, owing to the fact that the depletion zone for a particle at a low volume fraction is large according to the expression $V_v^{-1/3} - 1$.

Coarsening systems evolve in time through dissipation of excess interfacial free energy. The smooth dissipation of interfacial area ($S_v = \Sigma_{i=1}^N R_i^2$) can also be assigned some kinetic descriptions as in [3], and as shown in Fig. 7 from simulations. The total interfacial area, being a smooth quantity as opposed to fluctuating average quantities, even for finite clusters, can readily be associated with a rate constant. From Fig. 7, we see that $S_v \sim t^{-1/3}$. The rate constant K_{s_v}, which is the slope of the plot, also increases with volume fraction as shown. The ratio of the slopes

$$K_{s_v}(0.2)/K_{s_v}(0.1) = K_{s_v}(0.1)/K_{s_v}(0.05) = 1.8 \pm 0.12.$$

This result is in agreement with the theory by Marsh and Glicksman [3]. Their theory predicts an almost linear relation between the interfacial area rate constants and volume fraction.

Influence of cluster shape and periodicity

The distribution of particles in a periodic array of cells was studied in an attempt to investigate periodic boundary conditions and edge effects, which are known to impose yet another coarsening length scale corresponding to the size of a unit cell in the array. We used the method outlined by Voorhees and Glicksman [10,11] in order to investigate the effect of periodicity on the kinetics of clusters. We carried out a simulation of the diffusion fields for the case of 110 and 1150 particles per cell in an array of 125 cubic cells. We specifically solved the multiparticle problem to monopolar order in the volume fraction range of 0.01 to 10^{-13}. The problem formulation involves defining a nondimensional lattice translational vector given by

$$\mathbf{r}_l = u\mathbf{a} + v\mathbf{b} + w\mathbf{c}, \tag{56}$$

where u,v,w are integers and **a**, **b**, and **c** are the translational vectors of the lattice. By defining a set of basis vectors

$$\mathbf{r}_i = \alpha_i \mathbf{a} + \beta_i \mathbf{b} + \gamma_i \mathbf{c}, \tag{57}$$

one can translate the monopole sources and sinks to any of the cells. Hence

$$\phi(\mathbf{r}) = \phi_\infty + \sum_{\mathbf{r}_l} \sum_{i}^{N'} \frac{B_i}{|\mathbf{r}_i + \mathbf{r}_l - \mathbf{r}|}, \tag{58}$$

where N' is the total number of independent sources in the basis. The lattice sums appearing in Eq. (58) can be convergently summed using Ewald's method. The details of the application of the boundary condition and the evaluation of the sums are well laid out in [10,11].

The deviations of the coarsening rates from TLS in Fig. 8 for the periodic array are found to be less than those for the spherical cluster and the perturbation result by about 10%.

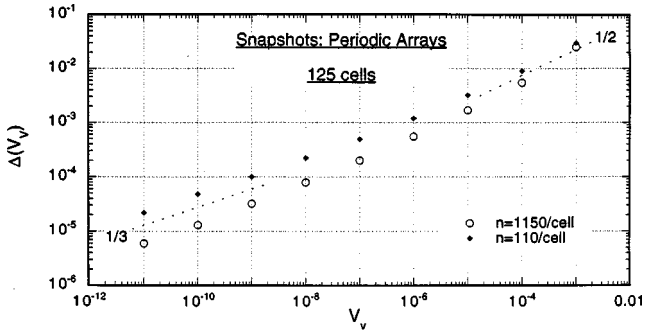

FIG. 8. Influence of cluster periodicity on deviations in coarsening rates from TLS.

This marginal decrease in the absolute value is due to a cluster shape effect. Even in this case, both $V_v^{1/2}$ and $V_v^{1/3}$ dependencies of the deviation are observed. The rollover volume fraction depends on the number of particles in a unit cell as

$$V_v^* \sim \frac{1}{12n^2},$$

as opposed to $(1/3n^2)$ found for the case of a spherical cluster. This difference is due to an edge effect, which is more pronounced in single spherical clusters. The particles close to the surface of the spherical cluster have fewer neighbors in all directions than those deep in the interior. The effective number of particles diffusionally interacting in the cluster is reduced and hence there is a slight departure from the prediction from Eq. (54), which does not account for any edge effects. We expect cluster edge effects to be less important for periodic arrays of clusters. The rollover volume fraction for periodic clusters $(1/12n^2)$, as expected, is closer to the theoretically predicted value of $(1/27n^2)$. Hence, periodicity does not significantly alter the volume fraction exponents of coarsening.

V. CONCLUSIONS

The snapshot numerical calculations presented here serve as an efficient method for computing the coarse-grained rate constants of finite clusters of coarsening particles at low volume fractions. The use of a large number of realizations significantly reduces fluctuations from the mean. In finite clusters the leading-order correction to the coarsening rate from TLS theory is $V_v^{1/3}$ as stated in [14]. The rollover volume fraction between the volume fraction exponents 1/2 and 1/3 at which the Debye screening distance becomes comparable to the cluster size depends on the number of particles considered. The dependence being $1/n^2$ suggests that large coarsening systems should not exhibit $V_v^{1/3}$ behavior. The simulations of the 3162 particles just reiterate this statement. The difference of $V_v^* = 1/27n^2$ and $V_v^* = 1/3n^2$ between theory and simulations indicates some edge effect. Inclusion of dipolar interactions becomes significant beyond a volume fraction of 0.01, with further deviations from Debye screening of the order V_v. The investigation of the rollover point from the $V_v^{1/2}$ behavior to linear behavior requires more robust numerical methods. Further investigations of the dependence of the rollover point on the number of particles need to be based on simulations of 10 000 particles and more.

At higher volume fractions spatial correlations begin to develop, and comprehensive time-dependent simulations yield higher coarsening rates than those from corresponding snapshot simulations. The ensemble averaging over *growing* particles alone is well justified heuristically by the $B(\rho)$ vs ρ plot. Other physically valid types of averaging such as surface area weighted averaging can also be used. The results thus obtained, however, are not expected to be significantly different from those presented here. The perturbation theory results of Fradkov *et al.* compare favorably with the direct time-dependent simulations reported here.

The effects of periodicity and cluster shape do not influence the volume fraction exponents of coarsening, but only alter the absolute values of the coarsening rates. Periodic arrays tend to reduce the cluster edge effects. The scaled particle size distributions from snapshot simulations are different from those predicted by time-dependent simulations. Spatial correlations, not incorporated into the snapshot calculations presented here, can have an influence on volume fraction exponents at higher volume fractions.

Our simulation results for the interfacial area coarsening rate confirm that K_{s_v} depends almost linearly on the volume fraction at low V_v. The nature of the time dependence for the coarsening of interfacial area, discussed by previous researches [37,38] is in agreement with that reported here.

Stochastic aspects of the problem can be investigated by considering the noise-functional nature of the $B(\rho)$. One can incorporate this information into the Fokker-Planck equation as done in [39] for infinite systems simplified by hierarchy equations. Preliminary calculations suggest that noise characteristics are considerably different in the early and late stage of phase separation [31]. Such noise effects can also help quantify important fluctuations in finite clusters. As expected in finite clusters, fluctuations and departures from continuum theory predictions may decrease with an increase in the number of particles in the cluster.

Future simulations using multipoles may incorporate higher-order terms such as quadrupoles, etc., at volume fractions higher than discussed here ($V_v \geqslant 0.3$). In this paper, particle shape change or centroid migration due to inclusion of dipole terms has not been considered in detail. Some researchers [15,37] have suggested that particles tend to migrate when surrounded by a nonspherically symmetric diffusion field, in order to remain spherical. The inclusion of quadrupole terms, however, would require consideration of shape change of particles. Future directions in simulations should also focus on structure factor development [32] and the effects of thermal noise associated with capillary phenomena.

ACKNOWLEDGMENTS

The authors gratefully acknowledge the financial support provided by the National Science Foundation, Washington D.C. under Grant No. DMR-9633346. The authors also thank Dr. G. B. McFadden, NIST, Gaithersburg, Maryland, and Professor L. Greengard, Courant Institute of Mathematical Sciences, NYU, New York, for their valuable suggestions on fast iterative solution methods for large linear systems.

[1] I. M. Lifshitz and V. V. Slyozov, J. Phys. Chem. Solids **19**, 35 (1961).
[2] O. M. Todes, J. Phys. Chem. Solids **20**, 629 (1946).
[3] S. P. Marsh and M. E. Glicksman, Acta Mater. **44**, 3761 (1996).
[4] A. J. Ardell, Acta Metall. **20**, 61 (1972).
[5] A. D. Brailsford and P. Wynblatt, Acta Metall. **27**, 489 (1979).
[6] S. P. Marsh and M. E. Glicksman, in *Modelling of Coarsening and Grain Growth*, edited by S. P. Marsh and C. S. Pande (TMS, Warrendale, 1989).
[7] J. H. Yao, K. R. Elder, H. Guo, and M. Grant, Phys. Rev. B **47**, 14 110 (1993).
[8] J. A. Marqusee and J. Ross, J. Chem. Phys. **80**, 536 (1984).
[9] M. Tokuyama and K. Kawasaki, Physica A **123**, 386 (1984).
[10] P. W. Voorhees and M. E. Glicksman, Acta Metall. **32**, 2001 (1984).
[11] P. W. Voorhees and M. E. Glicksman, Acta Metall. **32**, 2013 (1984).
[12] C. W. J. Beenakker, Phys. Rev. A **33**, 4482 (1986).
[13] M. Marder, Phys. Rev. A **36**, 858 (1987).
[14] V. E. Fradkov, M. E. Glicksman, and S. P. Marsh, Phys. Rev. E **53**, 3925 (1996).
[15] N. Akaiwa and P. W. Voorhees, Phys. Rev. E **49**, 3860 (1994).
[16] M. Hennion, D. Ronzaud, and P. Guyot, Acta Metall. **30**, 599 (1982).
[17] S. Abis *et al.*, Phys. Rev. B **42**, 2275 (1990).
[18] J. S. Pedersen, Phys. Rev. B **47**, 657 (1993).
[19] P. A. Rikvold and J. D. Gunton, Phys. Rev. Lett. **49**, 286 (1982).
[20] R. Triolo, E. Caponetti, and S. Spooner, Phys. Rev. B **39**, 4588 (1989).
[21] O. Krichevsky and J. Stavans, Phys. Rev. Lett. **70**, 1473 (1993).
[22] O. Krichevsky and J. Stavans, Phys. Rev. E **52**, 1818 (1995).
[23] R. T. Bonnecaze and J. F. Brady, Proc. R. Soc. London, Ser. A **432**, 445 (1991).
[24] M. Tokuyama and K. Kawasaki, Physica A **134**, 323 (1986).
[25] H. Reiss, H. L. Frisch, and J. L. Lebowitz, J. Chem. Phys. **31**, 1959 (1959).
[26] J. J. Weins and J. W. Cahn, in *Sintering and Related Phenomena*, edited by G. C. Kuczynski (Plenum, London, 1973), p. 151.
[27] P. W. Voorhees and R. J. Schaefer, Acta Metall. **2**, 327 (1986).
[28] E. D. Siggia, Phys. Rev. A **20**, 595 (1979).
[29] B. Widom, J. Chem. Phys. **44**, 3888 (1965).
[30] G. B. McFadden and L. Greengard (private communication).
[31] M. Tokuyama and Y. Enomoto, Phys. Rev. E **47**, 1156 (1993).
[32] H. Mandyam and M. E. Glicksman, Mater. Sci. Eng., A **238**, 121 (1997).
[33] A. Vrij, J. Chem. Phys. **71**, 3267 (1979).
[34] N. B. Mandayam and B. Aazhang, IEEE Trans. Commun. **43**, 229 (1995).
[35] S. Torquato, B. Lu, and J. Rubinstein, Phys. Rev. A **41**, 2059 (1990).
[36] H. Mandyam, M.S. thesis, Rensselaer Polytechnic Institute, 1997.
[37] T. Imaeda and K. Kawasaki, Physica A **164**, 335 (1990).
[38] T. Imaeda and K. Kawasaki, Mod. Phys. Lett. A **5**, 57 (1991).
[39] M. Tokuyama and Y. Enomoto, Physica A **220**, 261 (1995).